Macromolecules
ARTICLE

Macromolecules **2010**, *43*, 9937–9944 **9937**
DOI: 10.1021/ma102031k

Glassy Dynamics and Glass Transition in Nanometric Thin Layers of Polystyrene

Martin Tress,[†] Michael Erber,[‡] Emmanuel U. Mapesa,[†] Heiko Huth,[⊥] Jan Müller,[‡] Anatoli Serghei,[§,∥] Christoph Schick,[⊥] Klaus-Jochen Eichhorn,[‡] Brigitte Voit,[‡] and Friedrich Kremer*,[†]

[†]*Institute for Experimental Physics I, University of Leipzig, 04103 Leipzig, Germany,* [‡]*Leibniz-Institut für Polymerforschung Dresden e.V., 01069 Dresden, Germany,* [§]*Department of Polymer Science and Engineering, University of Massachusetts Amherst, Amherst, Massachusetts 01003, United States, and* [⊥]*Physics Institute, University of Rostock, 18051 Rostock, Germany.* [∥]*Present address: Université Lyon 1, CNRS, UMR 5223, Ingénierie des Matériaux Polymères, F-69622 Villeurbanne, France*

Received September 1, 2010; Revised Manuscript Received October 18, 2010

ABSTRACT: Broadband dielectric spectroscopy (BDS), spectroscopic vis-ellipsometry (SE), X-ray reflectometry (XRR), and alternating current (ACC) as well as differential scanning calorimetry (DSC) are combined to study glassy dynamics and the glass transition in nanometric thin (≥ 5 nm) layers of polystyrene (PS) having widely varying molecular weights (27 500−8 090 000 g/mol). For the dielectric measurements two sample geometries are employed, the common technique using evaporated electrodes and a recently developed approach taking advantage of nanostructures as spacers. *All* applied methods deliver the concurring result that deviations from glassy dynamics and from the glass transition of the bulk do not exceed margins of ±3 K *independent* of the layer thickness and the molecular weight of the polymer under study. Our findings are discussed in the context of the highly controversial literature and prove that an appropriate sample preparation is of paramount importance.

1. Introduction

The nature of the glass transition remains a subject of intense study for material as well as theoretical scientists. Several theoretical approaches[1−3] have been suggested to explain this phenomenon. The most recognized of these concepts is the idea of cooperative motion as empirically formulated by Adams and Gibbs.[1] Here, it is reasoned that for a sufficiently supercooled liquid, structural relaxation may occur if and only if a number of constituent molecules rearrange collectively. This cooperativity therefore suggests a certain length scale defining the cooperative region which grows with decreasing temperature. The existence of such a length scale of cooperative motion then points to finite size effects, that is, changes in the dynamics and glass transition temperature when the material is confined to length scales near the cooperative size. Such confinement can be achieved and studied using, *inter alia*, nanopores,[4] entangled polymers,[5] or thin films.[6] The latter provide an ideal sample geometry since the confinement dimension can be remarkably diminished by simply reducing the thickness of the films. Assuming the existence of finite size effects, the challenge then is quantifying a characteristic length scale for glass transition dynamics.

In their work on *cis*-polyisoprene, a material which exhibits two distinct modes (a segmental mode resulting from configurational transitions of a few monomer segments and a normal mode associated with the fluctuations of the end-to-end distance of the chain) of relaxation processes, Bahar et al.[7] showed that the length scale of the segmental relaxation and hence the structure size underlying the dynamic glass transition is just about three repeat units (polymer segments). This result is supported by many reports that find no shifts in the dynamic glass transition and no change of T_g down to film thicknesses of about 5 nm of polystyrene[8−19] and other polymers like poly(methyl methacrylate),[20] polysulfone,[21] or poly(2-vinylpyridine).[22] Nonetheless, there are contradicting results[23−39]—especially from ellipsometric measurements—ever since the first reports of Keddie et al.[23,24] on polystyrene and poly(methyl methacrylate).

In a recent work[19] on PS (M_w = 319 000 g/mol) studied by combined BDS and SE, we showed that—compared to bulk—glassy dynamics in layers as thin as ∼5 nm (BDS) and ∼20 nm (SE) is not shifted. In the current work—using similar annealing procedures (in inert gas atmosphere well above T_g for at least 12 h) for both techniques—we now extend this study to different molecular weights of polystyrene (27 000 < M_w < 8 090 000 g/mol) and probe the M_w dependence of the glassy dynamics. Further, we report in this article AC calorimetry (ACC) and X-ray reflectometry (XRR) measurements; the results are in quantitative agreement with the BDS and SE findings.

2. Experimental Details

2.1. Materials. Six different samples of atactic polystyrene (purchased from Polymer Standards Service GmbH) with varying molecular weights and polydispersity indices (Table 1) were studied by BDS and SE. Highly polished (monocrystal 100) silicon wafers (purchased from microFab and www.University-Wafer.com for BDS and SE, respectively) with a native oxide layer of about 2 nm were used as substrates for film preparation. These wafers have ultraflat surfaces (with a root-mean-square roughness better than 6 Å) and, in the case of the ones used for BDS experiments, a typical resistivity less than 5 mΩ cm. Glass (microscope) slides (Carl Roth GmbH & Co. KG) were also used as substrates in some of the BDS measurements. Toluene (99.9% pure) and acetone (99.8% pure) were used as solvents for film preparation and cleaning purposes, respectively, and were obtained from Sigma-Aldrich GmbH. Except for filtering (Millex syringe filters, PTFE membrane with 0.2 μm pore size)

*Corresponding author. E-mail: kremer@physik.uni-leipzig.de.

Published on Web 11/02/2010

Table 1. Characteristics of PS Samples Studied in This Work[a]

sample	M_w (kg/mol)	M_w/M_n	R_g (nm)
1	27.5	1.03	4.6
2	58.9	1.01	6.7
3	319	1.05	15.7
4	749	1.10	24.0
5	1103	1.14	29.1
6	8090	1.17	78.8

[a] Radii of gyration in Θ solvent were calculated according to the literature.[40]

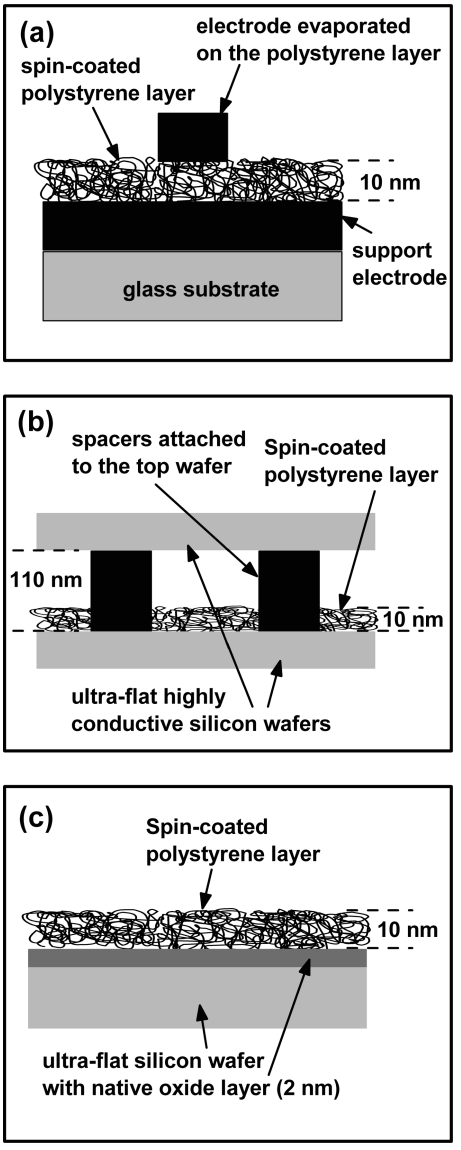

Figure 1. Schemes for the sample geometries applied for the dielectric and ellipsometric measurements: (a) capped geometry: use of evaporated aluminum electrodes; (b) uncapped geometry: novel approach where insulating silica nanostructures serve as spacers; and (c) geometry for ellipsometric measurements. Note: in (a) and (b) the native oxide layers on the electrodes are not shown for graphical clarity.

of the solutions before spin-casting, the polymer materials and solvents were used as received without further purification.

2.2. Sample Preparation. Regarding BDS measurements, two sample geometries were used. In the first geometry—the conventional approach—evaporated aluminum electrodes (thickness: ~80 nm; root-mean-square (rms) roughness: ≤1 nm) were used as counter electrodes as schematically represented in Figure 1a. The preparation and cleaning procedure we used is available in

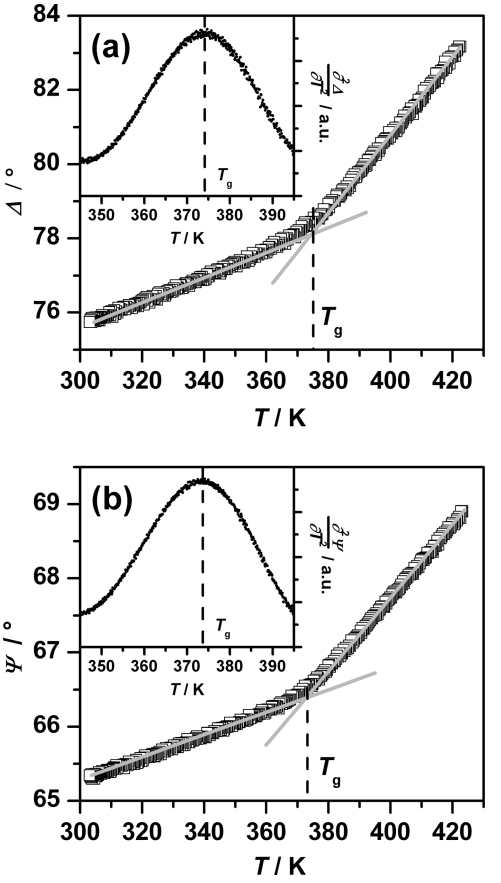

Figure 2. Ellipsometric angles ψ and Δ as functions of temperature for a 76 nm thin PS film (M_w = 319 000 g/mol) on native silicon oxide at a sensitive wavelength λ of 450 nm. The solid lines are a guide to the eye to illustrate the two linear regimes (glassy and rubbery) whose intersection point indicates the glass transition temperature T_g as highlighted by the dashed line. The insets show the second derivatives of the interpolated data (as described in the text), the maxima of which also occur at T_g.

the literature.[8] In the second geometry (Figure 1b) silicon wafers (rms roughness: ≤0.6 nm) were used as electrodes. Here, insulating silica nanostructures serve as spacers, keeping the two wafers separated by about 110 nm; a detailed description of this technique is published elsewhere.[41] For both geometries, the films were always annealed at 430 K (i.e., T_g + 50 K) for at least 24 h in oil-free high vacuum (10^{-6} mbar) before dielectric measurements. This treatment is necessary to remove any remaining solvent and to relax the chains after the spin-coating procedure.

For ellipsometric measurements, an alkaline cleaning procedure was used for purifying the silicon substrate surfaces. First, the wafers were cleaned in an ultrasonic bath of CH_2Cl_2 at room temperature for 15 min. Then, they were transferred to an alkaline hydroperoxide solution (Millipore water, resistivity ≥18 MΩ cm, H_2O_2 (30%) and NH_3 solution (25%) in the ratio 20:1:0.2) for 20 min at 354 K. Thereafter, the wafers were carefully rinsed by Millipore water, dried by argon flow, and directly used. The sample geometry used for SE measurements is shown in Figure 1c.

The layers (for both BDS and SE studies) were deposited by spin-casting at 3000 rpm for 20 s; the layer thickness was adjusted by varying the toluene−polystyrene concentration and determined by means of atomic force miscroscopy (AFM) to be within a variability of ±10% for layers down to ~20 nm and up to ±20% for thinner samples.

2.3. Measurement and Data Analysis. Dielectric measurements were carried out using a high-resolution Alpha analyzer and an Andeen−Hagerling impedance bridge; for both instruments, a Quattro temperature controller (Novocontrol Technologies) was used for temperature regulation, ensuring a relative

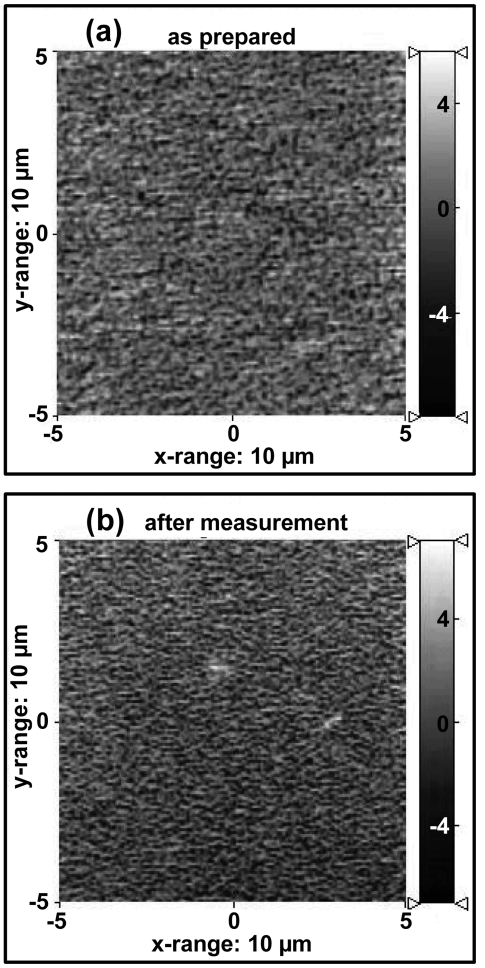

Figure 3. 10 by 10 μm^2 AFM pictures of the surface of a 5 nm thick PS film (M_w = 319 000 g/mol) on a silicon wafer as-prepared (a) and after the annealing (at 430 K for 24 h in oil-free high vacuum) and measurement (in a dry nitrogen atmosphere) procedure (b), with root-mean-square roughnesses of 2.0 and 1.7 nm, respectively.

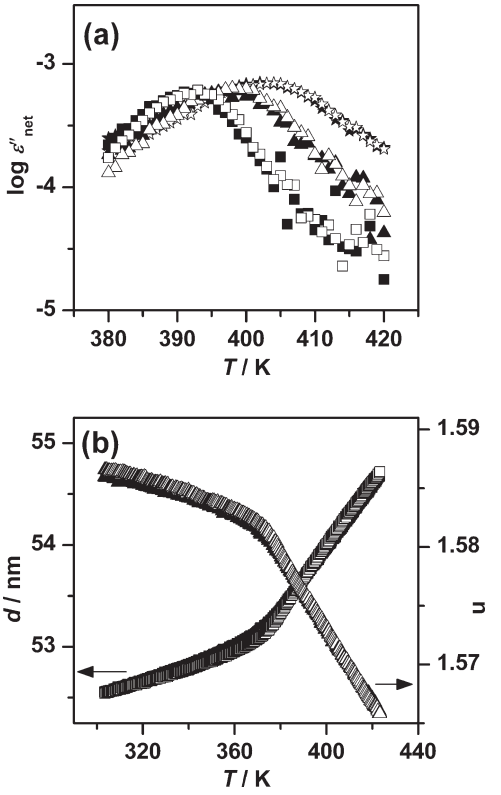

Figure 4. (a) Dielectric loss as a function of temperature at three frequencies [0.08 kHz (squares), 0.5 kHz (up triangles), 2 kHz (stars)] for an annealed 21 nm thin PS (1 103 000 g/mol) layer on a silicon wafer as recorded before (open symbols) and after (solid symbols) the substantive dielectric measurements. (b) Ellipsometrically determined thickness d and refractive index n of a 52 nm thin PS (M_w = 319 000 g/mol) sample during a typical heating (open symbols) and cooling (solid symbols) cycle are shown. The curves coincide (within a margin of ±3%), indicating reproducibility.

error of ≤0.1 K and an absolute error of < 1 K. Measurements were made in the frequency range 50 Hz−20 kHz at temperatures between 380 and 430 K. During measurement, samples were always kept in a pure nitrogen atmosphere. In a temperature representation of the dielectric spectra, the α-relaxation peak for polystyrene is clearly seen in the temperature window mentioned above. Therefore, we are able to obtain the characteristic (maximum loss) temperature T_α, at a chosen frequency, which effectively corresponds to the relaxation rate at this temperature.

Temperature-dependent spectroscopic ellipsometry measurements were carried out at a fixed angle of incidence (70°) using a multiwavelength (λ = 370−1680 nm) rotating compensator ellipsometer (RCE) M2000VI (J.A. Woollam Co., Inc.) connected to a closed heat cell (INSTEC Inc.). The real temperature on the surface of a silicon wafer was checked in a separate experiment by different melt transition standards from Perkin-Elmer (Sn, Pb, In, Zn) commonly used for calorimetry. The standards were melted to the wafer surface at appropriate temperature, then cooled, and reheated to record the melt transition and corresponding thermometer reading. By visually observing the consecutive melting points for the compounds at a ramp of 2 K/min, the temperature was checked within an accuracy of ±1 K in the temperature range 300−690 K. Recording of the ellipsometric data and heating/cooling were coordinated and controlled by software (Complete Ease, J.A. Woollam Co., Inc.). Real-time spectroscopic measurements were performed at a moderate scanning rate of 2 K/min. Annealing was carried out at 30 K above bulk (calorimetric) T_g under argon flow during which the thickness d and refractive index n of the sample were continuously monitored until sample stability was reached in about 15 h. Immediately after this treatment, the measurements for T_g determination were started under argon flow without exposing the samples to ambient air again. The layer thickness d and the refractive index n were calculated from the ellipsometric angles Ψ and Δ measured in the entire wavelength range assuming the layer stack Si/SiO_2/PS/ambient as optical model. A Cauchy dispersion (k = 0) for the wavelength dependence of the polymer refractive index $n(\lambda)$ was assumed. The temperature position of the discontinuity (commonly referred to as kink) in either $\psi(T)$ or $\Delta(T)$ (Figure 2) (or $d(T)$ or $n(T)$) is known to occur at the ellipsometric glass transition temperature. For better accuracy,[42] the extrema of interpolated curves of the second derivatives $\partial\psi^2/\partial T^2$ or $\partial\Delta^2/\partial T^2$ (or $\partial d^2/\partial T^2$ or $\partial n^2/\partial T^2$) (interpolation was done by applying a ninth-order polynomial fit) were used to determine T_g (Figure 2); values thus obtained in several heating and cooling cycles lie consistently within an error margin of ±2 K.

It should be noted that changes in the optical properties of the Si substrate with temperature can have significant impact on the accuracy of thickness determination in thin films.[43] Therefore, to evaluate the heating/cooling cycles, temperature-dependent data were used from the Woollam Complete Ease software[44] in which the optical properties of Si are stored as a function of temperature.

2.4. Reproducibility. For both BDS and SE measurements, AFM was applied to check the surface topography for as-prepared and annealed samples—before and after measurement

(see Figure 3). In order to exclude artifacts due to dewetting, only samples exhibiting a root-mean-square roughness less than 3 nm (on a lateral length scale of 10 μm) were considered for further analysis. To check the reproducibility of BDS results, the dielectric loss as a function of temperature was monitored (after annealing) before and after measurement (Figure 4a). Similarly, for SE several heating and cooling cycles were carried out on the samples after annealing and the data recorded as presented in Figure 4b (only one cycle is drawn for graphical clarity since the curves almost completely coincide). As shown in the aforementioned figures, reproducibility of results within a margin of ±3% is ascertained for both BDS and SE measurements.

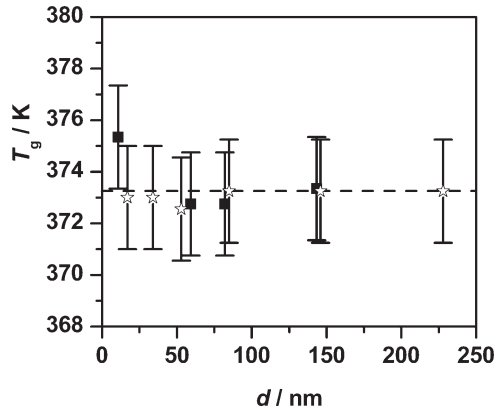

Figure 5. Thickness dependence of ellipsometrically determined T_g of PS layers (319 000 g/mol) supported on silicon substrates cleaned with acetone and dichloromethane in ultrasonic baths (squares) and an alkaline hydroperoxide solution (stars). Coinciding results prove the comparability of the two cleaning methods. The dashed line is a guide to the eye.

Despite differences in the substrate cleaning in the BDS and SE experiments (rinsing and ultrasonic cleaning with acetone and dichloromethane baths versus alkaline hydroperoxide solution, respectively), the obtained results are comparable. This is proven by additional SE measurements of PS layers (M_w = 319 000 g/mol) on silicon substrates which were cleaned in the identical way as done for BDS measurements. The thickness dependence of T_g of PS layers prepared on silicon substrates cleaned in either way is compared in Figure 5 and shows quantitative agreement. The T_g in the 10 nm thick layer on silicon cleaned with acetone and dichloromethane seems to be increased by about 2 K which compares to the error margin of the data.

2.5. Complementary Measurements. *2.5.1. AC Calorimetry.* AC calorimetry probes the frequency-dependent complex heat capacity which shows distinctive changes at phase transitions as well as the glass transition. A formerly developed differential AC-chip calorimeter[12−14] was applied to overcome the problem of very low sample mass in studying thin polymeric layers. Having a sensitivity of pJ/K, the calorimeter is capable of measuring sample masses below 1 ng and was shown to be suitable

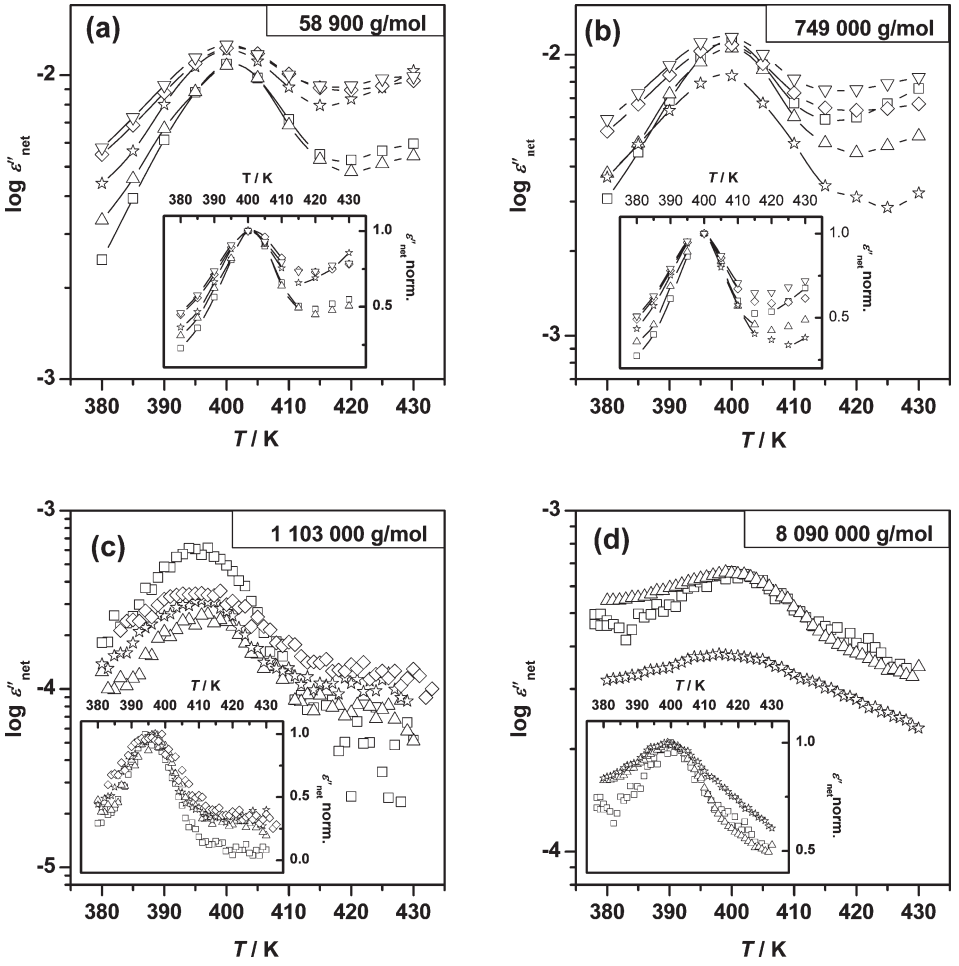

Figure 6. Temperature dependence of the dielectric loss ε''_{net} for samples prepared from four molecular weights of PS (as indicated) with varying layer thicknesses: (a) Measured at 1 kHz [169 nm (squares), 126 nm (up triangles), 72 nm (stars), 37 nm (diamonds), 29 nm (down triangles)]; (b) 0.5 kHz [171 nm (squares), 54 nm (up triangles), 35 nm (stars), 24 nm (diamonds), 17 nm (down triangles)]; (c) 0.24 kHz [91 nm (squares), 26 nm (up triangles), 21 nm (stars), 11 nm (diamonds)]; and (d) 1 kHz [29 nm (squares), 23 nm (up triangles), 9 nm (stars)]. The insets show the same curves normalized with respect to the maximum value of dielectric loss. *No* shifts in the temperature position of T_α are detected.

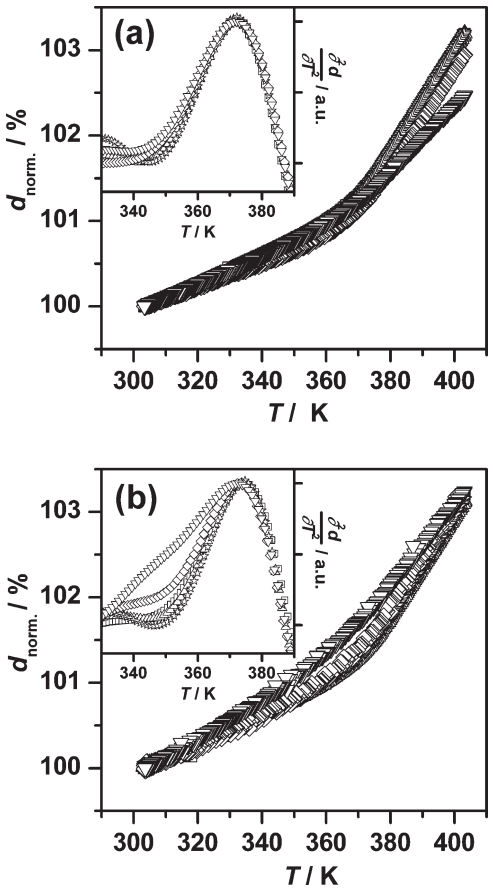

Figure 7. Ellipsometrically determined temperature dependence of the thicknesses d of PS layers normalized for layer thickness at 300 K for two molecular weights (a) 27 500 g/mol [thicknesses: 234 nm (squares), 121 nm (up triangles), 86 nm (stars), 54 nm (diamonds), 26 nm (down triangles)] and (b) 58 900 g/mol [thicknesses: 360 nm (squares), 138 nm, (up triangles), 59 nm (stars), 26 nm (diamonds), 12 nm (down triangles)]. The insets show the respective second derivatives of the interpolated data (ninth-order polynomial fits).

for the determination of the glass transition temperature in thin polymer layers.[12−16] Commercially available gas sensors suitable for fast scanning (XEN-39390 from Xensor Integration bv, Netherlands) having an effective sample area of about 30 × 30 μm^2 on a silicon nitride membrane (thickness ~1 μm) coated by a silica layer were employed in the differential setup.

The sample preparation was done (comparable to the previously described procedures) by spin-coating of toluene solutions of PS onto the sensors. Subsequently, the samples were annealed at 430 K for at least 24 h in oil-free high vacuum (10^{-6} mbar) and measured in a nitrogen atmosphere in a temperature range of 350−430 K at frequencies of 80 Hz and 1 kHz. The data were recorded during continuous heating and cooling at a rate of 1 K/min; for the analysis only data from the second heating and cooling cycle were used. In the investigated temperature range, the amplitude of the complex heat capacity exhibits a step while the phase shows a peak at the same position. The glass transition temperature is indicated by the half step heights or the maximum position of the peak (as exemplified in Figure A1). Before the extraction of the peak position by a Gaussian fit, the measured phase was corrected by a baseline subtraction.[45]

AFM measurements of the surface topology of the PS layers prepared on the calorimetry sensors revealed pronounced dewetting in thin samples (< 50 nm). This instability inhibited reasonable measurements, and consequently, AC calorimetry was only applied to study bulklike samples. Considering the successful preparation of thin layers on the other silica-coated substrates, a likely cause for the dewetting could be the roughness of the sensor which is comparably high (rms roughness of ~6 nm) and hence might initiate agglomeration.

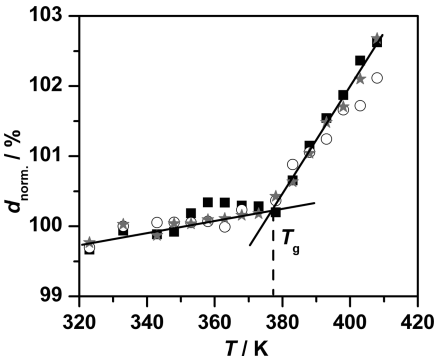

Figure 8. Temperature dependence of the normalized thickness d_{norm} of PS layers (M_w = 319 000 g/mol) having thicknesses of 35 nm (solid squares), 54 nm (open circles), and 87 nm (solid stars) as measured by XRR. The solid lines are linear fits to the data in the glassy and rubbery state for the 35 nm thick sample. The intersection point indicates the glass transition T_g.

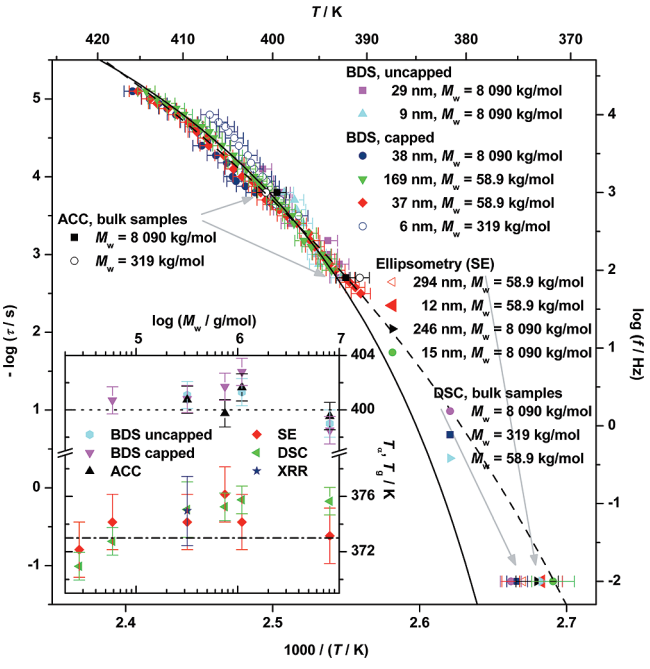

Figure 9. Activation plot of the mean relaxation rate of a selected set of measurements of various thickness and molecular weight samples as determined by several experimental methods as indicated. Within the error margins, the measurements carried out by BDS in two different sample geometries (capped and uncapped), AC calorimetry and DSC, are coinciding. Additionally, VFT fits to the data of two samples (M_w = 58 900 g/mol) having thicknesses of 169 nm (solid line) and 37 nm (dashed line) are displayed. The inset shows the molecular weight dependence of T_α as measured at a frequency of 1 kHz by BDS in uncapped and capped geometry and AC calorimetry as well as T_g determined by SE, XRR, and DSC for the thickest investigated samples (symbols as indicated). The dotted and dash-dotted lines at 400 and 373 K, respectively, are guides to the eye.

2.5.2. X-ray Reflectometry. X-ray reflectometry (XRR) is a surface-sensitive analytical technique suitable for determining the physical parameters of thin layers (about 1−100 nm). To do this, the superposition of reflected radiation with Bragg-like scattering effects caused by a layered structure is recorded. A more detailed description of this method is given elsewhere.[46−48] For our investigations, we used a XRD3003 T/T (Seifert FPM) with a copper anode. The X-ray beam was monochromated (Cu Kα, wavelength 1.54 Å), parallelized, and collimated to

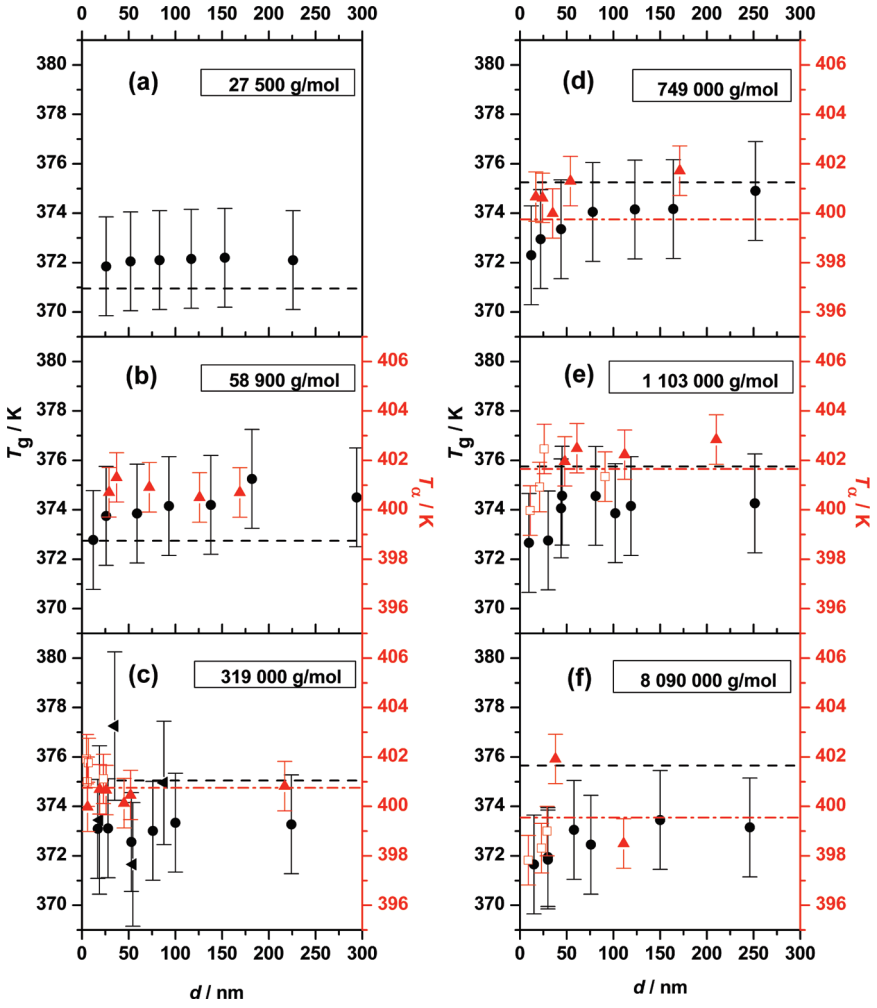

Figure 10. Temperature position (solid red up triangles show BDS measurements in capped geometry while open red squares are for measurements in uncapped geometry) of the α-relaxation peak T_α (right axes) in dependence of film thickness for different molecular weights as indicated measured at 1 kHz. Solid black circles represent the T_g values (left axes) as measured by ellipsometry, and the black left triangles in (c) display complementary measurements by XRR. Error margins are indicated as big as ±1 K for BDS, ±2 K for SE, and ±2.5 to ±3 K for XRR. For comparison, calorimetric measurements of bulk samples are shown: AC calorimetry (red dash-dotted line referring to the right axes) and DSC (black dashed line referring to the left axes). An enlargement of graph c showing the thickness range of 0−100 nm is given in Figure A2.

50 μm × 2 cm. The X-ray reflectivity was determined by specular reflection of the beam within low angles. By using the Parratt algorithm[49] (software: WIN-REFSIM), the reflectivity responses of the layer system on silicon substrate was simulated. As a result of simulation, we were able to determine the X-ray density, the layer thickness, and the roughness of the layer surface. For temperature-dependent measurements, we used a XRD Reactor Chamber (A. Paar KG) with two temperature controllers (Eurotherm 900). A cascaded temperature control with 5 °C steps was applied. After setting the temperature and before starting the measurement, we waited for stable temperature conditions. Inert gas atmosphere (helium) was used in order to prevent any oxidation. The temperature position of the glass transition (abrupt discontinuity in the thermal expansion, often referred to as "kink") was determined using the intersection point between two linear regressions of the glassy and rubbery state.

3. Results and Discussion

3.1. Broadband Dielectric Spectroscopy. The thickness dependence of the dynamic glass transition is shown in Figure 6 for PS layers having different molecular weights: 58 900 g/mol at 1 kHz (measured in capped geometry), 749 000 g/mol at 0.5 kHz (capped geometry), 1 103 000 g/mol at 0.24 kHz (uncapped geometry) and 8 090 000 g/mol at 1.0 kHz (uncapped geometry). Down to a thickness of 29 nm for PS 58 900 g/mol, 17 nm for 749 000 g/mol, 11 nm for 1 103 000 g/mol, and 9 nm for 8 090 000 g/mol, no shifts—as compared to bulk—in the dynamic glass transition are observed. Similar findings are observed for PS 319 000 g/mol (not shown in this figure) down to 4.8 nm.

The high-temperature wings in Figure 6a,b are conductivity contributions. The apparent broadening of the relaxation time distribution function observed in this data is attributed to oxide layers (of about 3 nm on aluminum[50] and 2 nm on silicon[51]) that are known to form on the substrates immediately the surfaces are exposed to air. An extensive and detailed discussion of the contributions of these oxide nanolayers as well as the sensitivity of the two methods to artifactual effects is available elsewhere.[19,52]

3.2. Ellipsometry. Ellipsometric measurements on PS for different molecular weights show clear discontinuities in the determined temperature dependences of the layer thickness (Figure 7) due to the transition from the glassy to rubberlike state; the explicit positions of these "kinks" are determined as already described in section 2.3. Within the error margins, no thickness dependence of the (ellipsometrically determined) T_g is exhibited by PS layers down to ∼20 nm for all the investigated molecular weights.

Table 2. Shifts of T_g and T_α for (Supported) Layers of PS as Reported in the Literature[a]

author (year)	experimental method	M_w [kg/mol]	d [nm]	mean shift of T_g/T_α [K]	substrate
Keddie[24] (1994)	ellipsometry	501	12	−25	H-passivated Si
		2900	12	−25	H-passivated Si
Forrest[27] (1997)	ellipsometry	767	29	−7	SiO_x
Ge[25] (2000)	AFM (shear force spectroscopy)	65	20	+5	SiO_x
		6500	20	+5	SiO_x
Tsui[36] (2001)	X-ray reflectometry	96	11	−15	SiO_x
Fukao[37] (2001)	thermal expansion spectroscopy/BDS	280	11	−20	Al (cap)
		6670	12	−8	Al (cap)
Efremov[11] (2004)	DSC	120	3	0	Pt
		10200	3	0	Pt
Fakhraai[35] (2005)	ellipsometry	641	6	−32	Pt
Ellison[31] (2005)	fluorescence spectroscopy	440	13	−35	glass
		3000	13	−35	glass
Lupascu[15] (2005)	BDS	160	5	+10	Al (cap)
Huth[13] (2006)	AC calorimetry	160	8	0	SiO_x
Raegen[33] (2008)	ellipsometry	734	25	0	SiO_x
			6	−50	SiO_x
Serghei[16] (2008)	BDS	700	12	0	Al (cap)
Mapesa[19] (2010)	BDS	319	5	+1 (±1)	SiO_x
		319	6	−1 (±1)	Al (cap)
	ellipsometry	319	17	0 (±2)	SiO_x
this study	BDS	1103	11	−2 (±1)	SiO_x
		749	17	+1 (±1)	Al (cap)
	ellipsometry	1103	10	−2 (±2)	SiO_x
		749	12	−2.5 (±2)	SiO_x
	X-ray reflectometry	319	19	−1 (±3)	SiO_x

[a] Only a few results are chosen from each study for reasons of brevity, and the selection is restricted to samples having a $M_w \geq 30\,000$ g/mol. The mean shifts of T_g and T_α at the denoted thicknesses are taken from diagrams so the values are approximated. In the last column the supporting material having direct contact with the polymer is specified; "SiO_x" refers to the native oxide layer of a silicon substrate while "H-passivated Si" describes an etching procedure which removes the native oxide and generates a hydrogen-passivated surface. "Al (cap)" indicates samples sandwiched between evaporated aluminum layers; otherwise, the polymer layers are not capped.

3.3. Calorimetry and X-ray Reflectometry. AC calorimetry was only employed to determine the T_g of thick (bulklike) samples. In the inset of Figure 8 the T_g as measured by AC calorimetry at 1 kHz is plotted versus molecular weight; in the range studied here, *no* molecular weight dependence is established for T_α. On the contrary, the T_g as measured by DSC reduces by about 7 K with decreasing molecular weight.

X-ray reflectometry was applied to measure thin layers (20−88 nm) of PS of a molecular weight of 319 000 g/mol. In all investigated samples the temperature dependence of the recorded layer thickness shows a distinct discontinuity indicating the glass transition temperature (exemplified in Figure 8). The measurements reveal *no* thickness dependence of T_g within the error margins of ±3 K and coincide with the ellipsometrically determined T_g values as displayed in graph c of Figure 10.

3.4. Summary and Comparison. The mean relaxation rate as measured by various experimental techniques versus inverse temperature is displayed in Figure 9 for a selection of the investigated samples. This shows, over a range of more than 2 decades of relaxation rate, that both sample geometries applied in the BDS experiments deliver coinciding results which are in full agreement with the AC calorimetry measurements. *No* deviation from the bulklike glassy dynamics in layers down to 5 nm is revealed in these measurements. Further, ellipsometry and X-ray reflectometry deliver coinciding T_g values which are in good agreement with the DSC measurements and the expected T_g extrapolated by fitting a Vogel−Fulcher−Tammann (VFT) equation[53−55] to the BDS data.

In the inset of Figure 9 the T_α and T_g values of bulklike samples as determined by the experimental techniques employed in this study are plotted versus molecular weight. Again, the coincidence of BDS and ACC measurements and the absence of a molecular weight dependence are shown. Similarly, the T_g values of the bulk as measured by ellipsometry, X-ray reflectometry, and DSC are in agreement, but in contrast to the first two, the results obtained by DSC exhibit a T_g reduction of about 5 K with decreasing molecular weight.

Figure 10 summarizes the experimental results for all the six molecular weights investigated in this work. Here, the thickness dependencies for the temperature position of the α-relaxation peak T_α (as measured by BDS at specified frequencies) and for T_g (as measured by SE) are explicitly shown. It is clear that alterations of dielectrically determined T_α and ellipsometrically determined T_g are mostly within the error margins of ±1 and ±2 K, respectively, and never exceed a difference of ±3 K from the thickest (bulklike) sample. However, it is remarkable that in four of the six investigated molecular weights (58 900, 749 000, 1 103 000, and 8 090 000 g/mol) there are slight thickness dependencies in T_g though within the error margins. With decreasing layer thickness, the T_g reduces instead of being randomly scattered around the bulk value. In contrast, this trend is not observed in an intermediate molecular weight of 319 000 g/mol which hinders the general conclusion of a thickness dependent shift of T_g. In summary, we prove that down to layer thicknesses of 5 nm the glassy dynamics is not altered by more than ±3 K over a wide range of molecular weights of polystyrene.

In comparing our results with the respective literature, agreement[8−18] but as well pronounced differerences[24−39] are reported; for the latter, shifts of T_g in dependence on the film thickness[24−37] and on the molecular weight[37−39] are observed. What could be the reason for this discrepancy? It is well-known that the segmental dynamics of a polymer and hence the dynamic and calorimetric glass transition are influenced by a variety of different effects: (i) remaining solvent acting as plasticizer in the polymer causes a pronounced increase in the segmental mobility,[56] (ii) physical aging,[8,9] and (iii) chemical degradation[9] shift as well the dynamic glass transition. Evidently these factors play an especially important role in

nanometric thin polymer layers as demonstrated in detail by Serghei and Kremer.[57] Recently, Perlich et al.[58] studied the solvent content in thin spin-coated PS homopolymer layers by neutron reflectrometry and found in freshly prepared samples (before annealing) a pronounced thickness and molecular weight dependence. Annealing for 8 h in vacuum (10^{-2} mbar) at a temperature of 20 K above T_g reduced the solvent content by only 1.0 vol % while at 60 K above T_g a 3.2 vol % effect was observed. Furthermore, an enrichment of solvent at the polymer/substrate interface was revealed. In view of these multiple parameters influencing the dynamic glass transition, it is not surprising that the shifts in T_g reported in the literature vary a lot (Table 2). It is most likely that this is due to artifacts of preparation.

4. Conclusion

In this work, the dynamic and calorimetric glass transition in nanometer-thin layers of PS having molecular weights between 27 500 and 8 090 000 g/mol has been investigated by multiple experimental techniques such as BDS, SE, XRR, DSC, and AC calorimetry. The glassy dynamics and the glass transition temperature under conditions of one-dimensional confinement in thin polymer layers are found to be independent of the molecular weight and of the layer thickness ($\geq$5 nm) within margins of $\pm$3 K.

Acknowledgment. The authors are grateful for funding by DFG (SPP 1369 and EI 317/4-1). Furthermore, the authors thank Liane Häussler for carrying out the DSC measurements.

Supporting Information Available: Figures A1 and A2. This material is available free of charge via the Internet at http://pubs.acs.org.

References and Notes

(1) Adam, G.; Gibbs, J. H. *J. Chem. Phys.* **1965**, *43*, 139.
(2) Cohen, M. H.; Grest, G. S. *Phys. Rev. B* **1979**, *20*, 1077.
(3) Götze, W.; Sjögren, L. *Rep. Prog. Phys.* **1992**, *55*, 241.
(4) Iacob, C.; Sangoro, J. R.; Papadopoulos, P.; Schubert, T.; Naumov, S.; Valiullin, R.; Kärger, J.; Kremer, F., *Phys. Chem. Chem. Phys.* **2010**, *12*, 13798.
(5) Rizos, A. K.; Ngai, K. L. *Phys. Rev. E* **1999**, *59*, 612.
(6) Hartmann, L.; Fukao, K.; Kremer, F. In *Broadband Dielectric Spectroscopy*; Kremer, F., Schönhals, A., Eds.; Springer: Berlin, 2003; pp 433−473.
(7) Bahar, I.; Erman, B.; Kremer, F.; Fischer, E. *Macromolecules* **1992**, *25*, 826.
(8) Serghei, A.; Kremer, F. In *Progress in Colloid and Polymer Science*; Grundke, K., Stamm, M., Adler, H.-J., Eds.; Springer: Berlin, 2006; pp 33−40.
(9) Serghei, A.; Huth, H.; Schellenberger, M.; Schick, C.; Kremer, F. *Phys. Rev. E* **2005**, *71*, 061801.
(10) Liu, Y.; Russell, T. P.; Samant, M. G.; Stöhr, J.; Brown, H. R.; Cossy-Favre, A.; Diaz, J. *Macromolecules* **1997**, *30*, 7768.
(11) Efremov, M. Y.; Olson, E. A.; Zhang, M.; Zhang, Z.; Allen, L. H. *Macromolecules* **2004**, *37*, 4607.
(12) Huth, H.; Minakov, A.; Schick, C. *Netsu Sokutei* **2005**, *32*, 69.
(13) Huth, H.; Minakov, A.; Schick, C. *J. Polym. Sci., Part B: Polym. Phys.* **2006**, *44*, 2996.
(14) Huth, H.; Minakov, A. A.; Serghei, A.; Kremer, F.; Schick, C. *Eur. Phys. J.: Spec. Top.* **2007**, *141*, 153.
(15) Lupascu, V.; Huth, H.; Schick, C.; Wübbenhorst, M. *Thermochim. Acta* **2005**, *41*, 222.
(16) Serghei, A.; Huth, H.; Schick, C.; Kremer, F. *Macromolecules* **2008**, *41*, 3639.
(17) Robertson, C. G.; Hogan, T. E.; Rackaitis, M.; Puskas, J. E.; Wang, X. *J. Chem. Phys.* **2010**, *132*, 104904.
(18) Weber, R.; Zimmerman, K.-M.; Tolan, M.; Stettner, J.; Seeck, O. H.; Erichsen, J.; Zaporojtchenko, V.; Strunskus, T.; Faupel, F. *Phys. Rev. E* **2001**, *64*, 061508–1.
(19) Mapesa, E. U.; Erber, M.; Tress, M.; Eichhorn, K.-J.; Serghei, A.; Voit, B.; Kremer, F. *Eur. Phys. J.: Spec. Top.* **2010**, *189*, 173.
(20) Erber, M.; Tress, M.; Mapesa, E.; Serghei, A.; Eichhorn, K.-J.; Voit, B.; Kremer, F. *Macromolecules* **2010**, *43*, 7729.
(21) Labahn, D.; Mix, R.; Schönhals, A. *Phys. Rev. E* **2009**, *79*, 011801.
(22) Serghei, A. *Macromol. Chem. Phys.* **2008**, *209*, 1415.
(23) Keddie, J. L.; Jones, R. A. L.; Cory, R. *Faraday Discuss. Chem. Soc.* **1994**, *98*, 219.
(24) Keddie, J. L.; Jones, R. A. L.; Cory, R. *Europhys. Lett.* **1994**, *27*, 59.
(25) Ge, S.; Pu, Y.; Zhang, W.; Rafailovich, M.; Sokolov, J.; Buenviaje, C.; Buckmaster, R.; Overney, R. M. *Phys. Rev. Lett.* **2000**, *85*, 2340.
(26) Wallace, W. E.; van Zanten, J. H.; Wu, W.-L. *Phys. Rev. E* **1995**, *52*, 3329.
(27) Forrest, J. A.; Dalnoki-Veress, K.; Dutcher, J. R. *Phys. Rev. E* **1997**, *56*, 5705.
(28) Fryer, D.; Nealey, P.; Pablo, J. *Macromolecules* **2000**, *33*, 6439.
(29) Tsui, O. K. C.; Zhang, H. F. *Macromolecules* **2001**, *34*, 9139.
(30) Kawana, S.; Jones, R. *Phys. Rev. E* **2001**, *63*, 02150.
(31) Ellison, C. J.; Mundra, M. K.; Torkelson, J. M. *Macromolecules* **2005**, *38*, 1769.
(32) Koh, Y. P.; McKenna, G. B.; Simon, S. L. *J. Polym. Sci., Part B: Polym. Phys.* **2006**, *44*, 3518.
(33) Raegen, A. N.; Massa, M. V.; Forrest, J. A.; Dalnoki-Veress, K. *Eur. Phys. J. E* **2008**, *27*, 375.
(34) Yang, Z.; Fujii, Y.; Lee, F. K.; Lam, C.-H.; Tsui, O. K. C. *Science* **2010**, *328*, 1676.
(35) Fakhraai, Z.; Forrest, J. *Phys. Rev. Lett.* **2005**, *95*, 025701.
(36) Tsui, O. K. C.; Russell, T. P.; Hawker, C. J. *Macromolecules* **2001**, *34*, 5535.
(37) Fukao, K.; Miyamoto, Y. *Phys. Rev. E* **2001**, *64*, 011803.
(38) Santangelo, P. G.; Roland, C. M. *Macromolecules* **1998**, *31*, 4581.
(39) Fukao, K.; Miyamoto, Y. *Phys. Rev. E* **2000**, *61*, 1743.
(40) Terao, K.; Mays, J. W. *Eur. Polym. J.* **2004**, *40*, 1623.
(41) Serghei, A.; Kremer, F. *Rev. Sci. Instrum.* **2008**, *79*, 026101.
(42) Erber, M.; Khalyavina, A.; Eichhorn, K.-J.; Voit, B. *Polymer* **2010**, *51*, 129.
(43) Kahle, O.; Wielsch, U.; Metzner, H.; Bauer, J.; Uhlig, C.; Zawatzki, C. *Thin Solid Films* **1998**, *313*, 803.
(44) Complete EASE Software Manual Version 3.18, J.A. Woollam Co., Inc., 2007.
(45) Weyer, S.; Hensel, A.; Schick, C. *Thermochim. Acta* **1997**, *305*, 267.
(46) Meyer, D. C.; Paufler, P. In *Encyclopedia of Nanoscience and Nanotechnology*; Nalwa, H. S., Ed.; American Scientific Publishers: Los Angeles, 2004; Vol. *10*.
(47) Gutmann, E.; Meyer, D. C.; Levin, A. A.; Paufler, P. *Appl. Phys. A: Mater. Sci. Process.* **2005**, *81*, 249.
(48) Chason, E. In *In Situ Real-Time Characterisation of Thin Films*; Auciello, O., Krauss, A. R., Eds.; John Wiley & Sons, Inc.: New York, 2000.
(49) Parratt, L. G. *Phys. Rev.* **1954**, *95*, 359.
(50) Konstadinidis, K.; Thakkar, B.; Chakraborty, A.; Potts, L.; Tannenbaum, R.; Tirrell, M. *Langmuir* **1992**, *8*, 1307.
(51) Morita, M.; Ohmi, T.; Hasegawa, E.; Kawakami, M.; Ohwada, M. *J. Appl. Phys.* **1990**, *68*, 1272.
(52) Serghei, A.; Tress, M.; Kremer, F. *J. Chem. Phys.* **2009**, *131*, 154904.
(53) Vogel, H. *Phys. Z.* **1921**, *22*, 645.
(54) Fulcher, G. S. *J. Am. Chem. Soc.* **1925**, *8*, 3701.
(55) Tammann, G.; Hesse, G. *Z. Anorg. Allg. Chem.* **1926**, *156*, 245.
(56) Zorn, R.; Monkenbusch, M.; Richter, D.; Alegria, A.; Colmenero, J.; Farago, B. *J. Chem. Phys.* **2006**, *125*, 154904.
(57) Serghei, A.; Kremer, F. *Macromol. Chem. Phys.* **2008**, *209*, 810.
(58) Perlich, J.; Körstgens, V.; Metwalli, E.; Schulz, L.; Georgii, R.; Müller-Buschbaum, P. *Macromolecules* **2009**, *42*, 337.